Membrane-Anchored Cytochrome c_y Mediated Microsecond Time Range Electron Transfer from the Cytochrome bc_1 Complex to the Reaction Center in *Rhodobacter capsulatus*[†]

Hannu Myllykallio,[‡] Friedel Drepper,[§,||] Paul Mathis,[§] and Fevzi Daldal*,[‡]

Department of Biology, Plant Science Institute, University of Pennsylvania, Philadelphia, Pennsylvania 19104, and Section de Bioénergétique, CNRS, URA 2096, DBCM, CEA Saclay, 91191 Gif-sur-Yvette, France

Received December 19, 1997; Revised Manuscript Received February 26, 1998

ABSTRACT: In *Rhodobacter capsulatus*, the soluble cytochrome (cyt) c_2 and membrane-associated cyt c_y are the only electron carriers which operate between the photochemical reaction center (RC) and the cyt bc_1 complex. In this work, cyt c_y mediated microsecond time range electron transfer kinetics were studied by light-activated time-resolved absorption spectroscopy using a mutant strain lacking cyt c_2. In intact cells and in isolated chromatophores of this mutant, only ∼30% of the RCs had their photooxidized primary donor rapidly rereduced by cyt c_y. Of these 30%, about half were reduced with a half-time of ∼5 μs attributed to preformed complexes, and the other half with a half-time of ∼40 μs attributed to cyt c_y having to move from another site. This slower phase was affected by addition of glycerol, indicating its dependence on the viscosity of the medium. Cyt c_y, despite its rereduction by ubihydroquinone oxidation in the millisecond time range, remained virtually unable to deliver electrons to other RCs which stayed photooxidized for several seconds. Furthermore, using two flashes separated by a variable time interval, it was shown that the fast electron donating complex was reformed in about 60 μs, a time span probably reflecting electron transfer from cyt c_1 to cyt c_y. In the absence of the cyt bc_1 complex, the steady-state level of cyt c_y in the chromatophore membranes obtained using cells grown in minimal medium was decreased to ∼50%. The remaining cyt c_y, however, was able to form the fast electron donating complex with the RC (half-time of ∼5 μs), whereas the slower phase with a half-time of ∼40 μs was strongly decelerated. This finding suggests a role for the cyt bc_1 complex in stabilizing cyt c_y and providing its "other" site, possibly via a close association between these components. Taken together, it is concluded that although cyt c_y is present in substoichiometric amount compared to the RCs, it supports efficiently photosynthetic growth of *R. capsulatus* in the absence of cyt c_2 because it can mediate fast electron transfer from the cyt bc_1 complex to the RC during multiple turnovers of the cyclic electron flow.

Multisubunit membrane components of photosynthetic and respiratory electron transport chains are generally connected to each other by smaller electron carriers. In the purple, nonsulfur bacteria of *Rhodobacter* species that offer an excellent model system for studying electron-transfer reactions, photosynthesis is driven by cyclic electron transport through the photochemical reaction center (RC)[1] and the ubihydroquinone:cytochrome (cyt) *c* oxidoreductase (cyt bc_1 complex). The RC is an integral membrane protein complex that carries the primary donor (P) and a chain of electron acceptors where the light-induced charge separation across the membrane takes place (*1*). Within the lipid bilayer, electron flow from the RC to the cyt bc_1 complex is mediated by ubihydroquinone, which is able to diffuse between the membrane-bound complexes (*2*). The secondary electron donor which rereduces P^+ from the periplasmic side of the cytoplasmic membrane is usually a *c*-type cytochrome (*3*), like the tetraheme subunit of *Rhodopseudomonas viridis* or the soluble (cyt c_2) or membrane bound (cyt c_y) monoheme cyt *c* of *Rhodobacter capsulatus* (for reviews, see refs *4* and *5*). Cyt c_2 can form a transient complex with the RC, which allows fast electron transfer (half-time of about 1 μs) to P^+. The kinetics of this reaction have been studied in detail using intact cells (*6*, *7*) or isolated RCs (*8*−*12*).

The photosynthetic (Ps) growth of a wild-type *Rhodobacter sphaeroides* strain is dependent on the presence of cyt c_2 as a secondary electron carrier (*13*) while that of *R. capsulatus* continues in its absence (*14, 15*). In the latter species, a membrane-bound cytochrome, termed cyt c_y,

[†] This work was supported by DOE Grant DE-FG02-91ER20052 to F. Daldal. F. Drepper was supported by a fellowship from the European Community.

* To whom correspondence should be addressed. Phone: (215) 898 4394. Fax: (215) 898 8780. E-mail: fdaldal@sas.upenn.edu.

[‡] University of Pennsylvania.

[§] CNRS.

[||] Current address: Albert Ludwigs Universität Freiburg, Biologisches Institut II, Schänzlestrasse 1, D-79104 Freiburg, Germany.

[1] Abbreviations: cyt, cytochrome; cyt bc_1 complex, ubihydroquinone: cyt *c* oxidoreductase; FCCP, *p*-trifluoromethoxycarbonylcyanidephenylhydrazone; LHI, light-harvesting complex I; MOPS, 3-(*N*-morpholine)propanesulfonic acid; N, amino; P, primary donor; Ps, photosynthetic; Q_A and Q_B, primary and secondary quinone acceptors of the RC, respectively; Q_o, ubihydroquinone oxidizing site of the cyt bc_1 complex; RC, reaction center; SD, standard deviation; SDS−PAGE, sodium dodecyl sulfate−polyacrylamide gel electrophoresis; TMBZ, 3,3′,5,5′-tetramethylbenzidine; TMPD, *N*,*N*,*N*′,*N*′,-tetramethyl-*p*-phenylenediamine.

S0006-2960(97)03123-1 CCC: $15.00
Published on Web 04/03/1998

Table 1: *Rhodobacter* Strains Used

strain	genotype	relevant phenotypes	ref
SB1003	Rif^R	wild-type	46
MT-1131	*crtD*121 Rif^R	wild-type[a]	47
MT-G4/S4	*crtD*121 Rif^R Δ(*cycA::kan*)	cyt c_2^-, Ps^+	14
MT-GS18	*crtD*121 Rif^R Δ(*cycA::kan*) Δ(*fbcBC::spe*)	cyt c_2^-, cyt bc_1^-, Ps^-	48
FJ2	*crtD*121 Rif^R Δ(*cycA::kan*) Δ(*cycY::spe*)	cyt c_2^-, cyt c_y^-, Ps^-	16
pFJ631/FJ2	*pRK415-cycY*/ *crtD*121 Rif^R Δ(*cycA::kan*) Δ(*cycY::spe*)	cyt c_y in trans in FJ2, cyt c_2^-,Tet^R, Ps^+	18
pHM12/MT-1131	*PcycY::lacZ*/ *crtD*121 Rif^R	cyt c_y*::lacZ* fusion in MT-1131, Ps^+	18
pHM12/MT-GS18	*PcycY::lacZ*/ *crtD*121 Rif^R Δ(*cycA::kan*) Δ(*fbcBC::spe*)	cyt c_y*::lacZ* fusion in MT-GS18, Ps^-	This work
pHM11/MT-1131	*pRK415-cycY*$_{188}$*::phoA*/ *crtD*121 Rif^R	cyt c_y*::phoA* fusion at position 188 in MT-1131, Ps^+	18
pHM11/MT-GS18	*pRK415-cycY*$_{188}$*::phoA*/ *crtD*121 Rif^R Δ(*cycA::kan*) Δ(*fbcBC::spe*)	cyt c_y*::phoA* fusion at position 188 in MT-GS18, Ps^-	This work
pHM10/MT-1131	*pRK415-cycY*$_{49}$*::phoA*/ *crtD121* Rif^R	cyt c_y*::phoA* fusion at position 49 in MT-1131, Ps^+	18
pHM10/MT-GS18	*pRK415-cycY*$_{49}$*::phoA*/ *crtD*121 Rif^R Δ(*cycA::kan*) Δ(*fbcBC::spe*)	cyt c_y*::phoA* fusion at position 49 in MT-GS18, Ps^-	This work

[a] MT-1131 is referred to as "wild-type" in this work since it is wild-type in terms of the growth phenotypes and cytochrome *c* profile.

functions as an alternate electron donor to the RC (*16*, *17*). Thus, in *R. capsulatus* two independent electron-transfer pathways capable of connecting the RC and the cyt bc_1 are present (*17*). *R. capsulatus* cyt c_y has recently been purified to homogeneity by epitope tagging (*18*), and its detailed characterization established that it is composed of two domains (*16*, *18*). Its amino (N)-terminal subdomain contains a hydrophobic uncleaved signal sequence which anchors to the membrane a carboxyl (C)-terminal domain highly homologous to mitochondrial cytochromes *c* (*18*). The membrane anchor and the cyt *c* domains are separated by a linker of about 70 residues rich in alanine and proline residues. Thus, *R. capsulatus* cyt c_y is a member of a growing subclass of membrane-bound *c*-type cytochromes (*16*, *19*, *20*, *21*). Most of these cytochromes [e.g., cyt c_{552} of *Paracoccus denitrificans* (*22*, *20*)] operate in respiratory electron transport with the exception of *R. capsulatus* cyt c_y, which is functional both in photosynthesis (*16*) and respiration (*23*). Interestingly, *R. sphaeroides* also contains a homologue of cyt c_y of unknown function (*21*). It seems unlikely that this cytochrome takes part in photosynthetic electron transport since a cyt c_2^- mutant of *R. sphaeroides* is Ps^- (*13*), although it can be complemented to Ps^+ growth by *R. capsulatus* cyt c_y (*24*). The ability of *R. capsulatus* cyt c_y to function both in respiration and photosynthesis makes it an attractive model for investigating the function of membrane-anchored electron carriers in general.

Previous spectroscopic and biochemical studies using several *R. capsulatus* strains (*17*) indicated that the absence of the cyt bc_1 complex affects both the oxidation kinetics and steady-state levels of cyt c_y in cytoplasmic membranes. Here, we used cyt c_2^- and cyt c_2^- cyt bc_1^- mutants of *R. capsulatus* to analyze in detail the properties of photosynthetic electron transport mediated by cyt c_y. For the first time, we were able to fully resolve the microsecond kinetics of electron donation from cyt c_y to the primary donor after its photooxidation by short flashes in both intact cells and chromatophores. These studies revealed that cyt c_y mediated electron transfer is as fast as that mediated by cyt c_2 and, furthermore, that it is fully functional during shortly spaced multiple turnovers. The electron-transfer properties of cyt c_y are compatible with its possible supramolecular organization with the cyt bc_1 complex in the context of the proposed structural model for the RC and its surrounding antenna complexes (*25*, *26*).

EXPERIMENTAL PROCEDURES

Bacterial Strains and Growth Conditions. The *R. capsulatus* strains used in this work are described in Table 1. Measurements with whole cells and chromatophores were performed using cells grown "semiaerobically" either in enriched MPYE medium or in Sistrom's minimal medium A (*27*) as described earlier (*16*). "Fully aerobic" cell cultures were obtained with vigorous shaking and using culture volumes not exceeding 10% of maximal capacity of culture flasks. Molecular genetic techniques have been described previously (*14*, *18*).

Biochemical Techniques. Cell cultures were harvested by centrifugation and washed in 10 mM KCl and 20 mM MOPS, pH 7.0. For measurements with intact cells, they were resuspended in a minimal volume of the washing buffer and used directly. Chromatophores were prepared in the same washing buffer using a French pressure cell as described earlier (*28*, *18*). Protein concentrations were determined by the method of Lowry (*29*), and 16.5% SDS−PAGE was done as described (*30*, *18*). The *c*-type cytochromes were revealed via the peroxidase activity of their heme group using tetramethylbenzidine (TMBZ) and H_2O_2 as in ref *31*. For densitometric analysis, TMBZ stained gels were digitized using an AlphaImager 950 imaging system (Alpha Innotech, CA). Several protein concentrations were used to ensure that relative intensities of different *c*-type cytochromes, determined using NIH-image 1.54 software (DCRT, NIH), were within the linear range of the CCD camera used. Where indicated, 2.5 or 5 μM myxothiazol and 1 μM valinomycin plus 2 μM FCCP were used to inhibit the turnover of the cyt bc_1 complex and to uncouple membrane potential and proton gradient, respectively. Alkaline phosphatase and β-galactosidase activities in cell-free extracts of *R. capsulatus* were determined as described by Brickman and Beckwith (*32*) and Miller (*33*), respectively.

Light-Activated Absorption Spectroscopy. Flash-induced, time-resolved absorbance changes were measured essentially as described previously (*10*, *11*). Flash excitation with a 20 ns pulse at 694 nm was provided by a ruby laser, and kinetics of electron transfer were monitored at 1283 nm in the absorption band of P^+. An optical path length of 10 mm for the measuring light and 3 mm for the actinic light were used. For measurements with intact cells, 80 μL of a concentrated cell suspension were filled into a thin (1 mm)

cuvette placed at 45° to the measuring beam and the direction of the flash excitation light. Absorbance changes in the green spectral region were measured as described by Drepper and Mathis (*12*). The amplified signals were digitized using a Tektronix (RTD) transient recorder. The 2048 channels of the data memory were partitioned into segments with different sampling rates. In double flash experiments, two identical ruby lasers (pulse width 20 ns, 694 nm) were used for excitation, and the data memory of the transient recorder was partitioned into segments with different sampling rates such that the kinetics in the microsecond and the millisecond time range induced by each of the two flashes could be resolved. Unless otherwise specified, the kinetic transients are the results of single-flash measurements without averaging, except for experiments performed on intact cells where 2−8 individual signals were averaged. The absorption transients were fitted to a sum of exponentials using a modified Marquardt algorithm installed by Dr. P. Sétif. In general, the half-times and amplitudes for each exponential were determined in unrestricted fits, except for the final curve-fitting analysis of the signals induced by a series of two flashes. In that case, a constant half-time of the fast kinetic phase was assumed, and its value was kept at a mean value found in unrestricted fits. This procedure was applied in order to improve the accuracy in determination of the amplitudes of the individual kinetic phases. The validity of this approach was judged from the residuals computed from the data and the fitted curves (not shown). No systematic deviations were visible, and in general, the quality of the fit was not improved when the rate constant of the fast phase was varied.

RESULTS

Kinetics of P^+ Reduction in Intact Cells. The kinetics of P^+ reduction induced by a series of two saturating laser flashes were measured as the absorption changes in the band of P^+ at 1283 nm for intact cells of the strains MT-1131 (wild-type), pFJ631/FJ2 (cyt c_2^-), FJ1 (cyt c_y^-), and FJ2 (cyt c_2^- cyt c_y^-) (Figure 1, traces a−d). As previously reported for intact cells and for chromatophores missing cyt c_2 (*15*, *17*), in the presence of cyt c_y and in the absence of cyt c_2, only about 30% of total P^+ rereduction proceeds in the microsecond domain (Figure 1, trace b) (similar data were also obtained using the strain MT-G4/S4 (cyt c_2^-), not shown). After the first flash, two dominant kinetic phases indicating electron donation from cyt c_y to P^+ with half-times ($t_{1/2}$) of 4−5 μs and 40−50 μs, and each accounting for about 15% of the total amplitude, could be identified. The remaining 70% of P^+ decays very slowly with a characteristic time of typically several seconds (not shown in Figure 1). This slow decay is attributed to RCs being devoid of any secondary electron donor, and, presumably, in these RCs, back-reaction from the acceptor side or P^+ reduction by ascorbate occurred. The extent of rapid P^+ reduction after the second flash (trace b) indicates that reduced cyt c_y was rapidly recovered in the microsecond time scale as a secondary donor to the RC. For example, 200 μs after the second flash, the extent of P^+ reduction was about 90% of that observed at the same time interval after the first flash. This fast recovery of cyt c_y is analyzed in more detail later.

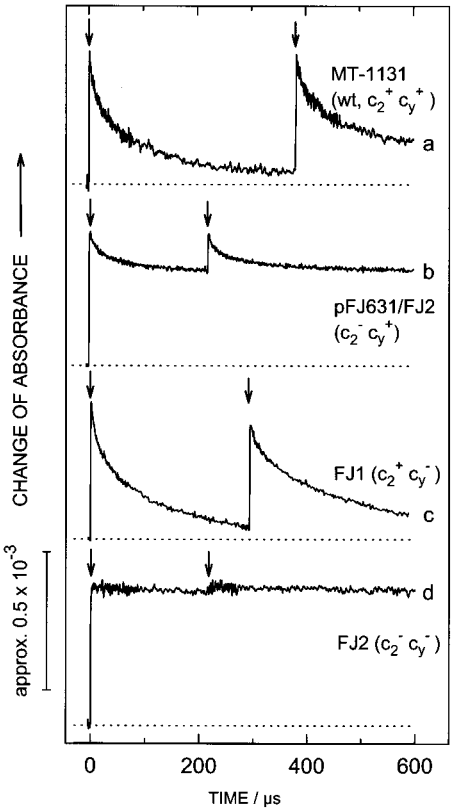

FIGURE 1: Absorption changes at 1283 nm of *R. capsulatus* intact cells of a wild-type strain (MT-1131, trace a) and strains missing cyt c_2 (pFJ631/FJ2, trace b), cyt c_y (FJ1, trace c) or both cyt c_2 and c_y (FJ2, trace d). Cells were resuspended in 10 mM KCl, 20 mM MOPS, pH 7.0, and 40 mM sodium ascorbate. Kinetics were induced by two saturating laser flashes delivered 380 μs (trace a), 290 μs (trace c), or 220 μs (traces b and d) apart, indicated by the vertical arrows.

Figure 1 also shows P^+ rereduction kinetics induced by cyt c_2 in the presence (trace a) or absence (trace c) of cyt c_y. A comparison of the kinetics of P^+ reduction in cells having only cyt c_y (Figure 1, trace b) with those having only cyt c_2 (Figure 1, trace c) as a secondary electron donor indicates that both the cyts c_y and c_2 reduced P^+ in a microsecond time range (detailed analyses of cyt c_2 mediated electron transfer will be presented elsewhere). In wild-type cells (Figure 1, trace a) about 90% of P^+ decayed within about 300 μs after the first flash. These kinetics show a complex behavior in the microsecond time domain, as expected due to the presence of both cyt c_2 and cyt c_y in these cells. Assuming that these electron-transfer pathways operate independently, it appears that in wild-type cells about 30% of P^+ was rereduced by cyt c_y and about 60% of P^+ by cyt c_2 in the microsecond time range. In the strain FJ2 missing both cyt c_2 and c_y (Figure 1, trace d), no rereduction of P^+ in the microsecond and millisecond time ranges was observed, in agreement with earlier reports (*34*, *35a*, *17*).

Kinetics of P^+ Reduction in Chromatophores. The kinetics of P^+ rereduction were also measured in chromatophores isolated from the strains MT-1131 (wild-type) and MT-G4/S4 (cyt c_2^-) (Figure 2) in the absence (dotted traces) or in the presence (solid traces) of 2.5 μM myxothiazol, a Q_o site inhibitor of the cyt bc_1 complex. In chromatophores of MT-G4/S4 (Figure 2B) or in pFJ631/FJ2 (data not shown) both lacking cyt c_2, P^+ reduction kinetics were similar to those observed in whole cells (Figure 1, trace b). In the micro-

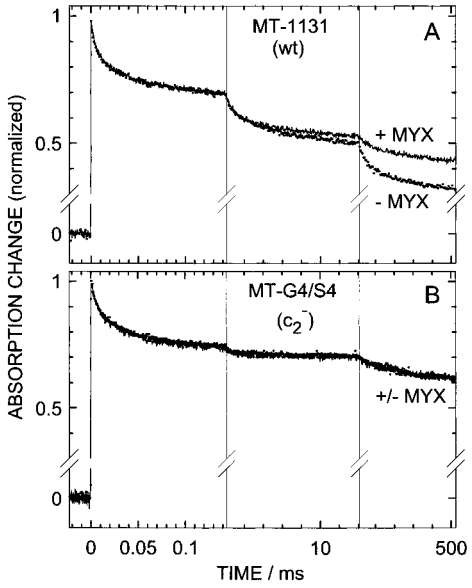

FIGURE 2: Kinetics of P^+ reduction in chromatophores from wild-type strain MT-1131 (A) and from cyt c_2 deletion strain MT-G4/S4 (B) monitored in the absence (dotted traces) or in the presence (solid traces) of 5 μM myxothiazol. Chromatophores were resuspended in 20 mM MOPS, pH 7.0, 4 mM sodium ascorbate at a final concentration of 20 OD units at 855 nm. Regions recorded with different sampling rates are separated by thin vertical lines. P^+ reduction was monitored as in Figure 1, and for MT-G4/S4, the two curves are superimposed. The signals are normalized to the amplitude of the initial flash-induced absorption change.

second time range, the kinetics of electron donation from cyt c_y to P^+ again exhibit two dominant phases with half-times ($t_{1/2}$) of 5 and 40 μs both having relative amplitudes of about 15% of the total signal. A minor contribution having a $t_{1/2}$ of 0.5−1 ms is clearly visible in Figure 2 and accounts for about 3% of total P^+. The remaining P^+ decays very slowly with a half-time of several seconds (not fully resolved in Figure 2) and is again attributed to the RCs being reduced by ascorbate or by back electron flow from Q_A or Q_B. By contrast, in chromatophores from wild-type (Figure 2A), the extent of P^+ rereduction in the microsecond time range is much smaller (about 35%) than that (about 90%) observed in intact cells (Figure 1, trace a), indicating that cyt c_2 was partly lost during the isolation of the chromatophores whereas the membrane-bound cyt c_y was not. Indeed, the microsecond kinetics in wild-type chromatophores (Figure 2A) resemble those in chromatophores from MT-G4/S4 (Figure 2B). However, additional kinetic components, which are absent in the kinetics of P^+ reduction by cyt c_y in MT-G4/S4, were observed in wild-type chromatophores. A small contribution (<10% relative amplitude) to the kinetics in the microsecond time range, a kinetic component with a $t_{1/2}$ of 1 ms (13%), and a slow kinetic component with a $t_{1/2}$ of 30 ms (15%) are present. The only difference between the strains used in these experiments being the presence of cyt c_2, these additional contributions are attributed to partial rereduction of P^+ by this cytochrome.

Cyclic Electron Transfer via cyt c_y. In chromatophores from both wild-type and MT-G4/S4 (cyt c_2^-) strains, the kinetics for time ranges shorter than 5 ms were not affected by addition of myxothiazol, an inhibitor of the Q_o site of the cyt bc_1 complex (Figure 2). On the other hand, only for the wild-type strain the slow kinetic component with a half-

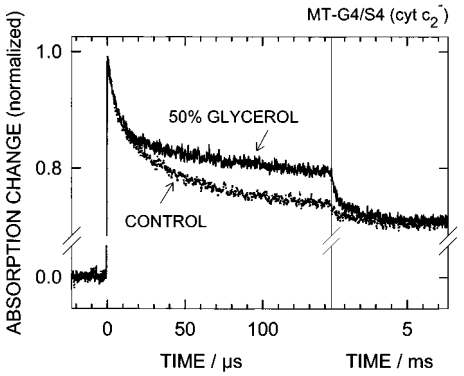

FIGURE 3: Kinetics of P^+ reduction induced by a laser flash in chromatophores isolated from the strain MT-G4/S4 (cyt c_2^-) measured in the presence (solid trace) and in the absence (dotted trace) of 50% (v/v) glycerol in the medium. Other conditions were as described in Figure 2, and the signals are normalized to the amplitude of the initial flash-induced absorption change. Note the expanded scale in the upper part of the ordinate axis for a better visualization of the μs and ms kinetics.

time of about 30 ms (dotted trace in the right panel of Figure 2A) disappeared almost completely upon addition of myxothiazol (solid traces). This indicates that, in the absence of myxothiazol, electrons rereducing cyt c_2 via oxidation of ubihydroquinone by the cyt bc_1 complex were delivered to some RCs that remained still in the P^+ state (obviously others than those already reduced by the cyts c_y and c_2 during the microsecond and millisecond kinetic phases following the flash). The myxothiazol-dependent phase of P^+ reduction was not observed when cyt c_y was the sole electron carrier (Figure 2B). Although in MT-G4/S4, 70% of the RCs remained in the P^+ state at 10 ms after the flash, these centers were not reduced by electrons coming through the cyclic electron transport pathway via ubihydroquinone and cyt bc_1 complex.

Effect of Glycerol on P^+ Rereduction. Measurements similar to those described above were carried out in the presence of varying amounts of glycerol in the chromatophore suspensions of MT-G4/S4 (Figure 3 and data not shown). When glycerol was added up to 50% (v/v), the rate and relative amplitude of the fast phase (i.e., $t_{1/2} \approx 5$ μs) of P^+ reduction were not changed while the rate of the slower phase (i.e., $t_{1/2} \approx 40$ μs under standard conditions) was markedly slowed. In the presence of 50% glycerol (Figure 3, solid trace), this latter phase reached a half-time of about 150 μs, indicating a strong effect of some physicochemical property of glycerol containing buffers. Using data obtained with various glycerol concentrations (not shown), this effect of glycerol was assumed to contribute to changes in the apparent viscosity as described in ref *35*(b), although additional dehydration effects cannot be excluded. The glycerol-independent fast phase was attributed to RCs with a preformed "proximal" complex with cyt c_y being competent in fast electron transfer to P^+ as it has been shown to be the case for cyt c_2 (reviewed in ref *4* and *5*). On the other hand, the glycerol (viscosity)-dependent slower phase presumably involves either a diffusional bimolecular reaction between the RC and cyt c_y or a reorientation of this cytochrome from an "other" position into a "proximal" one, where it is competent for rapid electron donation.

Reformation of the Cyt c_y−RC Complex. Excitation by two laser flashes given at variable time intervals was used

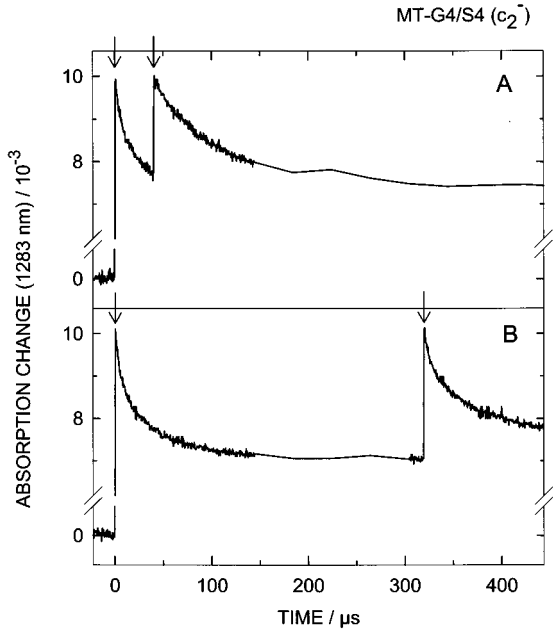

FIGURE 4: P^+ reduction kinetics in chromatophores from the strain MT-G4/S4 (cyt c_2^-) induced by two laser flashes given 40 μs (A) or 320 μs (B) apart. Experimental conditions were as in Figure 2 except that 20 μM TMPD was added. The positions of the flashes are indicated by vertical arrows, and the upper part of the ordinate axis is shown with an expanded scale for a better visualization of the μs kinetics.

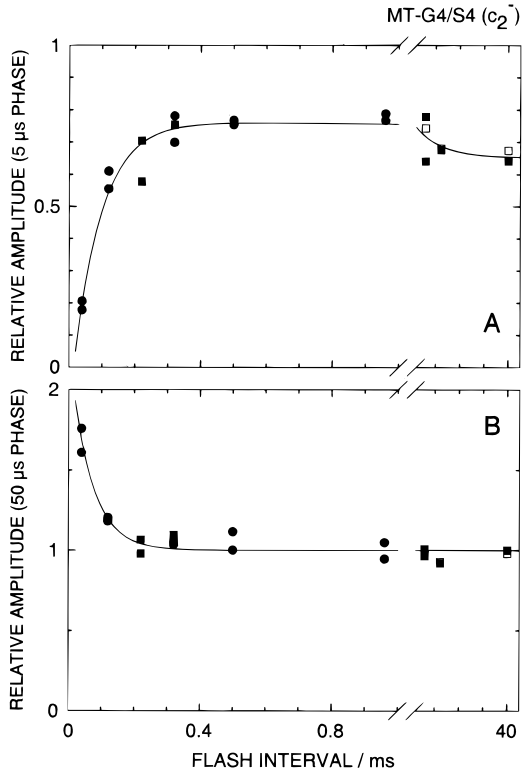

FIGURE 5: Relative amplitude of the fast ($t_{1/2} \approx 5$ μs, panel A) and the intermediate ($t_{1/2} \approx 50$ μs, panel B) kinetic components of P^+ reduction following a second flash as a function of the time interval between the first and the second flash. Chromatophores were from strain MT-G4/S4 (cyt c_2^-). Data obtained under the experimental conditions described in Figure 4 are indicated with filled circles. The data obtained in the absence of TMPD are shown with filled (no myxothiazol) and open (with 5 μM myxothiazol) squares. Data are given in units relative to the amplitude of the corresponding kinetic phase in the signal induced by the first flash. Calculated time courses are shown by solid lines (see the text and the Experimental Procedures for details).

to study the turnover of cyt c_y. Using chromatophores of MT-G4/S4 (cyt c_2^-), when the second flash was given at a relatively short interval of 40 μs after the first one, the kinetics of P^+ reduction in the microsecond time range showed an almost monophasic decay with a half-time of 50−60 μs (Figure 4A). By contrast, when the second flash was given at 320 μs after the first flash, the P^+ rereduction again exhibited a contribution from the faster ($t_{1/2} \approx 5$ μs) phase (Figure 4B). The level of photooxidation observed after the second flash given at a delay of 40 μs was similar to that seen after the first flash (Figure 4A), indicating that reoxidation of the primary quinone acceptor Q_A was almost complete during the 40 μs between the two flashes. A complete analysis of kinetic traces induced by a second flash given at varying time intervals after the first flash are summarized in Figure 5. For an accurate determination of the amplitudes of individual phases, the final curve-fitting analysis of the signals induced by the second flash was carried out using a constant value for the half-time of the fast phase as described in Experimental Procedures. The amplitude of the $t_{1/2} \approx 5$ μs phase as a function of the delay time between the first and the second flash is shown in Figure 5A. After a delay of about 300 μs, the amplitude of the fast phase after the second flash reached about 80% of that induced by the first flash, and corresponded almost to the maximal recovery in the millisecond time range. These data can be approximated by a fast exponential recovery with a $t_{1/2}$ of about 60 μs which has an extrapolated intercept with the abscissa of about 10 μs (solid line in Figure 5A). This intercept being greater than zero indicates that the data are consistent with a sigmoidal time course for delay times shorter than 40 μs. A slight decrease in the amplitude of the fast kinetic phase, the significance of which was not established, was observed for delay times between 1 and 40 ms. It is noteworthy that using the chromatophores of FJ1 (cyt c_y^-) excited by double flashes spaced by submillisecond time intervals, no comparable recovery of the fast phase indicative of a rereduction of the RC by cyt c_2 was observed (data not shown). Furthermore, in whole cells of FJ1 this recovery was about two to three times slower than the fast recovery seen in Figure 5A (F. Drepper, et al., unpublished experiments).

The amplitude of the slower phase ($t_{1/2} \approx 50$ μs) of the signal obtained after the second flash is shown in Figure 5B. The data are presented in units relative to the amplitude of the same kinetic phase observed after the first flash. The average half-time for this phase was slightly higher in the signals following the second flash (50 ± 5 μs) than for those seen after the first flash (40 ± 5 μs), and the solid line in Figure 5B is a fit of the data points to a single-exponential yielding a $t_{1/2}$ of 45 μs.

Possible contributions to the rereduction of cyt c_y in the submillisecond time range due to ubihydroquinone oxidation, or to TMPD used as a mediator, were also checked. Control experiments without any mediator are shown by filled squares, and those recorded in the presence of a saturating concentration of myxothiazol (2.5 μM) as a Q_o site inhibitor of the cyt bc_1 complex are shown by open squares. In these controls, no significant change in the amplitude of the

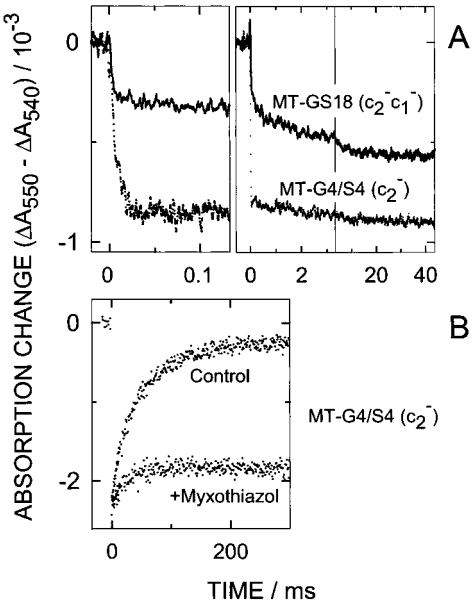

FIGURE 6: (A) Kinetics of flash-induced cytochrome *c* photooxidation in chromatophores isolated from the strains MT-GS18 (cyt c_2^- cyt c_1^-; solid traces) and MT-G4/S4 (cyt c_2^-; dotted traces) monitored as difference of the absorption changes measured at 550 and 540 nm. Kinetics were recorded with an electrical bandwidth of DC to 1 MHz (left graph) or DC to 100 kHz (right graph). (B) Effect of myxothiazol (Q_o site inhibitor of the cyt bc_1 complex) on the kinetics of cytochrome *c* rereduction in MT-G4/S4 (cyt c_2^-) chromatophores. Experimental conditions were as in Figure 2, except that the chromatophore concentrations were 10 (Figure 6A) or 20 (Figure 6B) OD units at 855 nm. Valinomycin (1 μM)/FCCP (2 μM) and 2.5 μM myxothiazol were used in all cases, except in the control measurement in Figure 6B which did not contain any myxothiazol. An average of six experiments were recorded at each wavelength with a dark interval of 3 min between the experiment.

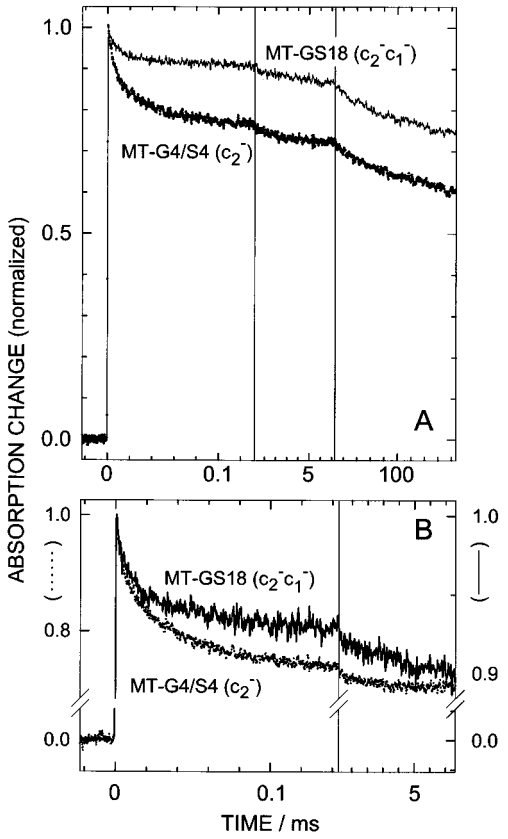

FIGURE 7: (A) Kinetics of P^+ reduction in chromatophores isolated from the strains MT-GS18 (cyt c_2^- cyt bc_1^-; solid traces) and MT-G4/S4 (cyt c_2^-; dotted traces). Experimental conditions were as in Figure 2. The signals are normalized to the amplitude of the initial flash-induced absorption change which, for MT-GS18, was 95% of that in MT-G4/S4 (approximately 0.01). In panel B the upper part of the ordinate axis is shown with an expanded scale for a better visualization of the μs kinetics. For comparison of the individual kinetic phases, the vertical axis for MT-GS18 (right ordinate in panel B) is expanded by a factor of 2.7 relative to that for MT-G4/S4 (left ordinate axis) in order to show the two traces with equal absolute sizes of the 5 μs phase (see the text for details).

microsecond kinetic phases was observed (Figure 5). Therefore, the observed rapid recovery of the fast P^+ reduction kinetics reflected electron transfer from cyt c_1 and the FeS center of the cyt bc_1 complex to cyt c_y and reformation of the RC−cyt c_y complex.

Why Myxothiazol Has No Effect on cyt c_y-Dependent Cyclic Electron Transfer? The data presented in Figure 2 indicate that horizontal exchange of electrons between the different cyt c_y independent cyclic electron transport chains does not take place as revealed by the lack of effect of myxothiazol when cyt c_2 is absent. However, to address directly the question of at which point this exchange is prevented, flash-induced kinetics of cyt *c* photooxidation and subsequent rereduction were also measured at 550 nm, where both cyts c_y and c_1 absorb similarly in their reduced state. Figure 6 shows the oxidation and subsequent reduction of cytochromes *c* (cyts c_y and c_1) in chromatophores from the strain MT-G4/S4, monitored as the difference of absorption changes at 550 and 540 nm. In Figure 6A, cyts *c* oxidation was recorded with microsecond (left panel) and millisecond (right panel) time resolution. The data indicate that the cyts *c* were oxidized in less than 100 μs, as suggested previously by Prince et al. (*15*). The time course observed with MT-G4/S4 (cyt c_2^-) (Figure 6A, dotted trace) was consistent with biphasic kinetics with $t_{1/2}$ of 3−5 μs and ∼20 μs, although the deconvolution of the kinetic components is less accurate in this case than in the P^+ reduction kinetics described above. Figure 6B indicates that the rereduction of the cyts c_y and c_1 occurred with a half-time of about 30 ms (control trace) and that this rereduction was sensitive to the cyt bc_1 complex inhibitor myxothiazol. Thus, the cyts c_1 and c_y were reduced by electrons flowing via the cyt bc_1 complex after about 100 ms as has been described previously (*15*, *17*, *34*). However, both in the whole cells (Figure 1; trace b) and chromatophores (Figure 2B), the fully reduced cyts c_y are unable to deliver electrons to other RCs which remain in the P^+ state for several seconds. These data clearly indicate that in vivo all functional cyt c_y are committed to interact solely with those RCs that are rapidly reduced in the microsecond time domain.

Cyt c_y Kinetics in the Absence of the cyt bc_1 Complex. The possibility that the cyt bc_1 complex plays a structural role in the formation of electron-transfer complexes between the RCs and cyts c_y has been suggested earlier (*17*). This possible role was further probed here by measuring the kinetics of the cyts c_y and c_1 oxidation (Figure 6A) and of P^+ reduction (Figure 7) in strains missing either the cyt c_2 (MT-G4/S4) or both the cyt c_2 and the cyt bc_1 complex (MT-GS18). For these experiments, chromatophores were from cells grown in Sistrom's minimal medium since cyt c_y is not detected in the absence of the cyt bc_1 complex on MPYE

grown cells (*17*). The kinetics of P^+ reduction in chromatophores from MT-GS18 (Figure 7A, solid trace), monitoring electron donation from cyt c_y to the RC in the absence of the cyt bc_1 complex, exhibited a fast phase with a half-time ($t_{1/2} \approx 5$ μs) similar to that seen in MT-G4/S4 (Figure 7A, dotted trace). However, its relative amplitude was decreased from about 15% in the presence of the cyt bc_1 complex to about 5% in its absence. A better comparison of these two signals is achieved by compensating this smaller amplitude by use of an expanded scale (Figure 7B). This comparison reveals that the $t_{1/2}$ of 40 μs phase observed in the presence of the cyt bc_1 complex (dotted trace) was markedly slowed ($t_{1/2} > 150$ μs) in its absence (solid trace). The fraction of P^+ reduced by the cyts c_y and c_1 within 40 ms after the flash was decreased from 30% of total P^+ in the presence of the cyt bc_1 complex (Figure 7A, MT-G4/S4, dotted traces) to approximately 15% in its absence (Figure 7A, MT-GS18, solid traces). The remainder of P^+ decayed very slowly ($t_{1/2} \approx 2$ s) and was not accompanied by the oxidation of cyts *c* (Figure 6A). A behavior quantitatively similar to those observed with P^+ reduction (Figure 7) is also visible in the kinetics of oxidation of cyt c_y and c_1 (Figure 6A, dotted traces) and cyt c_y (Figure 6A, solid traces) measured in chromatophores from MT-G4/S4 and MT-GS18, respectively. Again the amplitude of the fast phase ($t_{1/2} \approx 5$ μs) was diminished in the absence of the cyt bc_1 complex to about 40% of that found in its presence, and no ~20 μs phase was observed in the case of MT-GS18. Instead, a slower cyt c_y oxidation was completed within 40 ms after the flash, reaching an amplitude of only about 65% of that detected in MT-G4/S4.

Ratio of cyt c_y to cyt c_1 of the cyt bc_1 Complex. To gain further insight into the decreased amplitude of electron donation from cyt c_y to the RC in the absence of the cyt bc_1 complex, the steady-state amount of cyt c_y in chromatophores of the strains studied above was investigated by using TMBZ/SDS−PAGE. Densitometric analysis of such a gel indicates that the steady-state level of cyt c_y in cells grown semiaerobically in Sistrom's minimal medium was approximately 40−50% lower in MT-GS18 in comparison to that detected in MT-G4/S4 (Figure 8A, lanes 1 and 2). Moreover, considering that the β-galactosidase and alkaline phosphatase fusions to *cycY* encoding cyt c_y (*18*) exhibited similar amounts of activities in the presence and absence of the cyt bc_1 complex in these mutants (Table 2), it appears that the absence of the cyt bc_1 complex decreases postsecretionally the amount of cyt c_y in the cytoplasmic membranes, possibly by affecting its steady-state stability. In addition, these studies also reveal that the relative amounts of the cyts c_y and c_1 detected in cells grown by "fully" aerobic respiration or by anaerobic photosynthesis are different (Figure 8B). For example, "fully" aerobic cultures of SB1003, an isogenic parent of the strains used throughout this work, contained three to four times more cyt c_1 than cyt c_y, while its Ps cultures contained similar amounts of them. Finally, it is also noteworthy that, in Ps grown cells of *R. capsulatus*, the cyts c_p and c_o subunits of the cyt cbb_3 oxidase (*28*) are not detectable by TMBZ/SDS−PAGE (Figure 8B). These data clearly establish that, in *R. capsulatus*, the amounts of the membrane-bound *c*-type cytochromes are tightly regulated with the growth conditions used, and they should only be compared using cells grown under similar conditions.

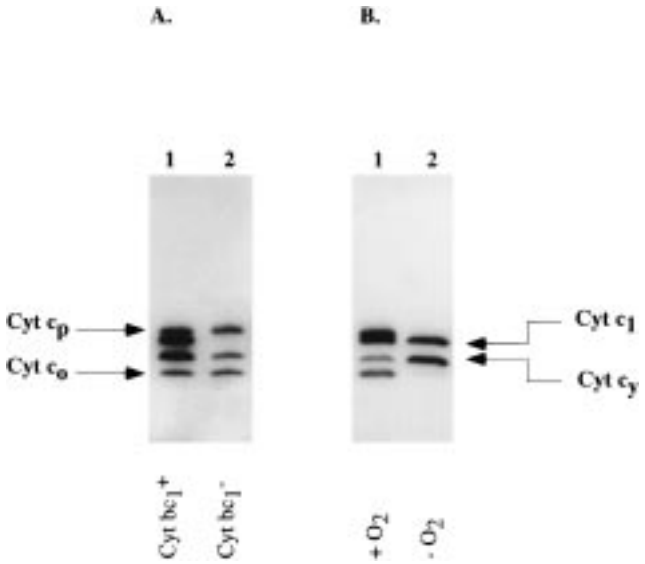

FIGURE 8: TMBZ/SDS−PAGE analysis of *c*-type cytochromes in various *R. capsulatus* strains. (A) Lane 1, MT-G4/S4 (cyt c_2^-); lane 2, MT-GS18 (cyt c_2^- cyt c^-). In each case, 50 μg of membrane proteins prepared from cells grown "semiaerobically" in Sistrom's minimal medium were used. (B) Lane 1, "fully aerobic" culture of SB1003; lane 2, Ps culture of SB1003. In each case, 75 μg of membrane proteins prepared from cells grown in enriched MPYE medium were used.

DISCUSSION

In this work, the pathway of cyclic electron transport via the membrane-anchored cyt c_y in *R. capsulatus* was studied in detail using mutants lacking the soluble cyt c_2. Kinetic data obtained and their analyses allowed a detailed interpretation of this electron transfer in terms of molecular reaction mechanisms. Previous kinetic studies have shown that a fraction of the RCs are connected to cyt c_y which functions as a rapid electron donor to P^+. However, prior to this work, this "fast phase" of cytochrome oxidation had not been resolved kinetically (*15*). Here, we have studied the single-turnover kinetics of electron donation from cyt c_y to the photooxidized RC (P^+) in the microsecond time range. In contrast with what we find for cyt c_2, the same kinetic behavior was found in cells and in chromatophores, indicating that cyt c_y was not lost during the preparation of chromatophore vesicles, in agreement with its membrane attachment. Further, excitation by a series of two flashes delivered at varying intervals was used to monitor the rereduction of cyt c_y and the reformation of the functional complex with the RC within cyclic electron transport through the cyt bc_1 complex. In addition, we have also demonstrated that the electron-transfer properties and the steady-state stability in the cytoplasmic membranes of cyt c_y are affected by the absence of the cyt bc_1 complex.

Docking and Electron Transfer from cyt c_y to the RC. The two kinetic phases of P^+ reduction by cyt c_y, with half-times of approximately 5 and 40 μs and accounting for 30% of the RCs, show striking differences. The fast phase ($t_{1/2} \approx 5$ μs) is attributed to electron donation within a "proximal" complex between the RC and cyt c_y since its rate and amplitude not depend on the viscosity of the medium. It is noteworthy that the same half-time, although with a smaller amplitude, was also observed in the absence of the bc_1 complex (Figure 7). Thus, the formation of a "proximal"

Table 2: Absence of the Cyt bc_1 Complex Does Not Affect the Expression of Cyt c_y

	β-galactosidase		alkaline phosphatase	
reporter construct	MT-1131 (wild-type)	MT-GS18 (cyt c_2^- bc_1^-)	MT-1131 (wild-type)	MT-GS18 (cyt c_2^- bc_1^-)
pHM12 (*cycY::lacZ*)	100 ± 3.8%[a]	112 ± 5.1%	ND[b]	ND
pHM10 ($cycY_{49}$*::phoA*)	ND	ND	100 ± 7.2%[c]	119 ± 9.7%
pHM11 ($cycY_{188}$*::phoA*)	ND	ND	100 ± 1.0%	136 ± 6.5%

[a] 100% corresponds to β-galactosidase activity (1688 ± 65.3 Miller units) (*33*) using strain MT-1131. Values given are an average of four independent measurements ± SD. [b] Not determined. [c] 100% corresponds to alkaline phosphatase activities in MT-1131 using either pHM10 (517 ± 37.3 units) or pHM11 (840 ± 7.3 units). Values were calculated using a formula described in ref *32* and are an average of four independent measurements ± SD.

RC−cyt c_y complex does not appear to depend on the presence of the cyt bc_1 complex. On the other hand, the second phase ($t_{1/2} \approx 40$ μs) was slowed both in the absence of the cyt bc_1 complex and upon addition of glycerol (i.e., with increasing viscosity), indicating a molecular movement as a rate-limiting process. This is interpreted as cyt c_y moving from "another" site, possibly in contact with the cyt bc_1 complex, into the "proximal" position before fast electron donation to P^+ can occur. An alternative interpretation of the $t_{1/2}$ of 40 μs phase is a bimolecular reaction between unbound cyt c_y and RC which have no cyt c_y bound prior to the flash. However, since under our experimental conditions cyt c_y is unable to reach about 70% of the RCs even in the time scale of seconds, its mobility relative to the RC appears to be limited, and consequently, we consider the latter interpretation unlikely. In addition, the former interpretation is also consistent with earlier findings where oxidation of cyt c_y was analyzed as a function of RC oxidation under conditions of varying excitation light intensity (*36*). These results also revealed that cyt c_y is essentially immobile relative to cyt c_2 within the microsecond time scale of these experiments.

Rapid Rereduction of cyt c_y within the Isolated Electron Transport Chains. Cytochrome *c* oxidation kinetics indicate that cyts c_y and c_1 are rereduced in less than 100 ms via the oxidation of ubihydroquinone by the cyt bc_1 complex ($t_{1/2} \approx 30$ ms) (Figure 6B). Yet, cyt c_y still remains unable to deliver these electrons to other RCs which remain in the P^+ state for several seconds, as revealed by the absence of any effect of myxothiazol on the kinetics of P^+ reduction (Figure 2B). Therefore, all functional cyt c_y is restricted to those RCs that are rapidly reduced in the microsecond kinetics.

In our studies, two kinetic processes which monitor the rapid delivery of a second electron by cyt c_y to the same RC were also resolved. First, the recovery of the amplitude of the fast phase induced by the second flash monitors the reformation of a functional complex between reduced cyt c_y and the RC. For this process the data obtained suggest a time course consistent with a short lag phase (~10 μs) and an exponential increase with a half-time of ~60 μs (Figure 5A). On the other hand, if a second flash is given after a time interval longer than what is needed for electron transfer within the "proximal" complex ($t_{1/2} \approx 5$ μs) induced by the first flash (e.g., after 40 μs), then almost monophasic kinetics of P^+ reduction with a half-time of 50−60 μs are observed (Figure 4A). Since this half-time is close to that of the 40 μs phase of P^+ reduction observed following the first flash, this latter phase can be expected to contribute to the apparently monophasic rereduction of P^+. Indeed, the amplitude of that phase is about 1.7-fold larger after the second flash than after the first flash. Thus, in addition to those P^+ that give rise to the 40 μs phase following the first flash, a large proportion of the RCs which had been rereduced during the 5 μs phase do also contribute to this phase with an effective $t_{1/2}$ of 50−60 μs after the second flash. This half-time therefore estimates the time for delivery of the second electron to the RCs in which two charge separations (i.e., two turnovers) have occurred. It is likely that both of the aforementioned processes reflect the same rate-limiting step, that is the movement of cyt c_y from the "other" position apparently close to the cyt bc_1 complex to the "proximal" position on the RC, resulting in the ~40 μs phase of P^+ reduction.

Role of the cyt bc_1 Complex for the Function of cyt c_y. Deletion of the cyt bc_1 complex has two effects on the kinetics of P^+ reduction by cyt c_y. The amplitude of the 5 μs phase decreases whereas the 40 μs phase decreases in amplitude and is slowed markedly. Both of these effects can be rationalized by the observation that the steady-state level of cyt c_y in MT-GS18 (cyt c_2^- bc_1^-) grown in Sistrom's minimal medium is 40−50% of that in MT-G4/S4 (Figure 8). Reporter gene studies indicate that the decreased steady-state level of cyt c_y in the absence of the cyt bc_1 complex is a postsecretional effect (Table 2), suggesting that in *R. capsulatus* the cyt bc_1 complex stabilizes cyt c_y, possibly by eliminating its degradation or decreasing its turnover via structural interactions.

Stoichiometry of the RC and the Secondary Donors. The data reported in this work provide biophysical and biochemical evidence that the cyt c_y pathway is organized in isolated electron-transport chains allowing rapid rereduction of P^+ by cyt c_y. In turn, cyt c_y is also rapidly rereduced by electrons originating from the cyt bc_1 complex, i.e., cyt c_1 and the FeS ("Rieske") center, as observed earlier (*17*, A. Vermeglio et al., unpublished experiments). A simple model that can account for such isolated electron-transfer chains working efficiently would involve a close association of stoichiometric amounts (i.e., 1 to 1 or 2 to 2) of RC and cyt c_y per cyt bc_1 complex. However, whether this situation is specific to *R. capsulatus* and cyt c_y or whether it also exists in other species is unknown. For example, in *R. sphaeroides*, whether the analogous electron transport via cyt c_2 occurs within isolated "supercomplexes" or involves a diffusion of cyt c_2 is currently debated. Joliot et al. (*6*, *37*) have proposed that in the latter species electron-transport chains form supercomplexes containing two RCs, one cyt c_2, and one cyt bc_1 complex. A different interpretation has been reported by Fernandez-Velasco and Crofts (*38*), who proposed a rapid equilibration of cyt c_2 between individual cyt bc_1 complexes. Furthermore, in *R. sphaeroides* the soluble isocyt c_2 has also

been described as an alternative secondary donor to the RC (*39*), but unlike the cyt c_2, it is not organized into kinetic supercomplexes (*40*).

To address the question of the stoichiometry between those RCs associated with cyt c_y and their secondary donors in *R. capsulatus*, the number of electrons that can be delivered to the RC in the submillisecond time range following one or two saturating flashes were quantified. The kinetic traces obtained using intact cells (Figure 1, trace b) and chromatophores (Figure 4B) revealed that the extent of P^+ reduction by cyt c_y following the second flash is clearly larger than half of that after the first flash. If the second flash is delivered at a delay time where P^+ reduction induced by the first flash is >90% completed (e.g., 220 μs in Figure 1b), the extent of P^+ reduction after this second flash approaches about 90% of that observed at the same time interval after one single flash. Assuming two RC, one cyt c_y, one cyt c_1, and one FeS center (i.e., 1.5 secondary donors per RC), the amount of P^+ reduction following a second flash would be at most 50% of that following one single flash. By contrast, in our experiments, over 1.9 secondary donors per RC in intact cells or chromatophores of the cyt c_2^- strains pFJ631/FJ2 and MT-G4/S4, respectively, were observed in the submillisecond time range. This value is too high to account for two RC, one cyt c_y, one cyt c_1, and one FeS center. Furthermore, no contribution from ubihydroquinone oxidation is visible in this time interval, since myxothiazol has no effect on the amplitude of P^+ reduction induced either by one (Figure 2B) or two flashes (Figure 5). Finally, in photosynthetically grown wild-type cells of *R. capsulatus*, approximately equal amounts of the cyts c_1 and c_y were found using TMBZ/SDS−PAGE (Figure 8B). The data taken all together support the presence of the same amounts of RC and cyt c_y per cyt bc_1 complex in isolated electron-transport chains in *R. capsulatus*. Clearly, isolation of the putative structural supercomplexes should shed further light to both their composition and the stoichiometry of their components.

Why some Photosynthetic Bacteria Have cyt c_y. One of the main findings of this work is that, due to its membrane attachment, the relative mobility of cyt c_y with respect to the RC and cyt bc_1 complex is limited in comparison to cyt c_2. In wild-type chromatophores, a kinetic phase of P^+ reduction, which is sensitive to myxothiazol, indicates that under our experimental conditions cyt c_2 is mobile, unlike cyt c_y (Figure 2). While this behavior of cyt c_2 is in agreement with the earlier reports suggesting that cyt c_2 can diffuse between several electron-transport chains in *R. sphaeroides* (*38*), that of cyt c_y is clearly different in that it is restricted to interact with a limited number of RCs. Yet, despite the relatively low amount of RCs connected to the cyt bc_1 via cyt c_y, these interactions provide efficient cyclic electron flow to support the Ps growth of *R. capsulatus* lacking cyt c_2 (*16*).

The observed electron-transfer properties of cyt c_y raise several interesting issues with respect to the recent structural models for the photosynthetic apparatus in purple bacteria (*41*). Analyses of two-dimensional crystals of dissociated subunits of light-harvesting complex I (LHI) (*25*) and units of LHI and RC complexes (*26*) indicate that LHI complexes are organized into ring-like structures in cytoplasmic membranes in *Rhodospirillum rubrum* and that the RC is centrally located within these structures. The interiors of these rings are large enough to accommodate a monomeric, but not dimeric, RC (*25*). Considering the large size of approximately 100 kDa of *R. capsulatus* cyt bc_1 complex (*42*), it seems unlikely that both the RC and the cyt bc_1 complex would be located within these structures. That the cyt bc_1 complex is located outside of these rings is in accordance with the observations that, in the presence of the LHI complex, a gene product of *pufX* is needed for an efficient exchange of ubiquinone/ubihydroquinone between the Q_B site of the RC and the cyt bc_1 complex in both *R. capsulatus* (*43*) and *R. sphaeroides* (*44*, *45*). Since the data presented in this work suggest close interactions between the cyt c_y and the cyt bc_1 complex, it could be proposed that the relatively long linker domain of *R. capsulatus* cyt c_y is to facilitate the movement of its cyt *c* domain across the LHI ring structures to mediate electron transfer between the complexes. It is noteworthy that the corresponding linker region of *R. sphaeroides* cyt c_y, which is unable to support Ps growth in both *R. sphaeroides* or *R. capsulatus* (Myllykallio and Daldal, unpublished observations), is considerably shorter in comparison to that of *R. capsulatus* cyt c_y. If this proposal is correct, then the shorter "linker" domain of *R. sphaeroides* cyt c_y may restrict its movement between the "proximal" and "other" positions of cyt c_y as described above, thus preventing electron transfer from the cyt bc_1 complex to the RC. In this respect, it was previously observed that in *R. capsulatus* a cyt c_2^- mutant is more impaired than its wild-type parent for Ps growth under nonsaturating light intensities (*14*), possibly reflecting that increased antenna sizes under these conditions restrict the access of cyt c_y to the RCs.

In summary, the work described here demonstrates that in *R. capsulatus* electron transfer from the cyt bc_1 complex to the RC via the membrane-attached cyt c_y is a fast process which functions efficiently during multiple turnovers of the cyclic electron-transport chain to sustain adequate Ps growth even in the absence of the soluble electron carrier cyt c_2. Further biochemical and structural studies are necessary to investigate the involvement of cyt c_y in the proposed structural complexes constituted of the RC and the cyt bc_1 complex.

ACKNOWLEDGMENT

We thank Drs. U. Liebl for valuable help during the experiments, R. C. Prince for helpful discussion, and A. Vermeglio for communicating to us his related findings prior to publication.

REFERENCES

1. Feher, G., and Okamura, M. Y. (1978) in *The Photosynthetic Bacteria* (Clayton, R. K., and Sistrom, W. R., Eds.) pp 349−386, Plenum Press, New York.
2. Crofts, A. R., and Wraight, C. A. (1983) *Biochim. Biophys. Acta 726*, 149−186.
3. Meyer, T. E., and Donohue, T. J. (1995) in *Anoxygenic Photosynthetic Bacteria* (Blankenship, R. E., Madigan, M. T., and Bauer, C. E., Eds.) pp 725−745, Advances in Photosynthesis, Kluwer Academic Publishers, Dordrecht, The Netherlands.
4. Tiede, D. M., and Dutton, P. L. (1993) in *The Photosynthetic Reaction Center* (Deisenhofer, J., and Norris, J. R., Eds.) pp 257−288, Academic Press, New York.
5. Mathis, P. (1994) *Biochim. Biophys. Acta 1187*, 177−180.

6. Joliot, P., Verméglio, A., and Joliot, A. (1989) *Biochim. Biophys. Acta 975*, 336−345.
7. Sabaty, M., Jappé, J., Olive, J., and Verméglio, A. (1994) *Biochim. Biophys. Acta 1187*, 313−323.
8. Tiede, D. M.. Vashishta, A.-C., and Gunner, M. R. (1993) *Biochemistry 32*, 4515−4531.
9. Wachtveitl, J., Farchaus, J. W., Mathis, P., and Oesterhelt, D. (1993) *Biochemistry 32*, 10894−10904.
10. Venturoli, G., Mallardi, A., and Mathis, P. (1993) *Biochemistry 32*, 13245−13253.
11. Drepper, F., Dorlet, P., and Mathis, P. (1997) *Biochemistry 36*, 1418−1427.
12. Drepper, F., and Mathis, P. (1997) *Biochemistry 36*, 1428−1440.
13. Donohue, T. J., McEwan, A. G., van Doren, S., and Crofts, A. C. (1988) *Biochemistry 27*, 1918−1925.
14. Daldal, F., Cheng, S., Applebaum, J., Davidson, E., and Prince, R. C. (1986) *Proc. Natl. Acad. Sci. U.S.A. 83*, 2012−2016.
15. Prince, R. C., Davidson, E., Haith, C. E., and Daldal, F. (1986) *Biochemistry 25*, 5208−5214.
16. Jenney, F. E., and Daldal, F. (1993) *EMBO J. 12*, 1283−1292.
17. Jenney, F. E., Prince, R. C., and Daldal, F. (1994) *Biochemistry 33*, 2496−2502.
18. Myllykallio, H., Jenney, F. E., Moomaw, C. R., Slaughter, C. A., and Daldal, F. (1997) *J. Bacteriol. 179*, 2623−2631.
19. Bott, M., Ritz, D., and Hennecke, H. (1991) *J. Bacteriol. 173*, 6766−6772.
20. Turba, A., Jetzek, M., and Ludwig, B. (1995) *Eur. J. Biochem. 231*, 259−265.
21. Zeilstra-Ryalls, J. H., and Kaplan, S. (1995) *J. Bacteriol. 177*, 6422−6431.
22. Berry, E. A., and Trumpower, B. L. (1985) *J. Biol. Chem. 260*, 2458−2467.
23. Hochkoeppler, A., Jenney, F. E., Lang, S. E., Zannoni, D., and Daldal, F. (1995) *J. Bacteriol. 177*, 608−613.
24. Jenney, F. E., Prince, R. C., and Daldal, F. (1996) *Biochim. Biophys. Acta 1273*, 159−164.
25. Karrasch, S., Bullough, P. A., and Ghosh, R. (1995) *EMBO J. 14*, 631−638.
26. Walz, T., and Ghosh, R. (1997) *J. Mol. Biol. 265*, 107−111.
27. Sistrom, W. (1960) *J. Gen. Microbiol. 22*, 778−785.
28. Gray, K. A. M., Grooms, M., Myllykallio, H., Moomaw, C., Slaughter, C., and Daldal, F. (1994) *Biochemistry 33*, 3120−3127.
29. Lowry, O., Rosebrough, A., Farr, A., and Randall, F. (1951) *J. Biol. Chem. 193*, 265−273.
30. Schägger, H., and von Jagow, G. (1987) *Anal. Biochem. 166*, 368−379.
31. Thomas, P. E., Ryan, D., and Levin, W. (1976) *Anal. Biochem. 75*, 168−176.
32. Brickman, E., and Beckwith, J. (1975) *J. Mol. Biol. 96*, 307−316.
33. Miller, J. H. (1972) in *Experiments in molecular genetics*, Cold Spring Harbor Laboratory, Plainview, NY.
34. Jones, M. R., McEwan, A. G., and Jackson, J. B. (1990) *Biochim. Biophys. Acta 1019*, 59−66.
35. (a) Zannoni, D., Venturoli, G., and Daldal, F. (1992) *Arch. Microbiol. 157*, 367−374. (b) Oh-Oka, H., Iwaki, M., and Itoh, S. (1997) *Biochemistry 36*, 9267−9272.
36. Jenney, F. E. (1994) Ph.D. Thesis, University of Pennsylvania, Philadelphia.
37. Joliot, P., Verméglio, A., and Joliot, A. (1996) *Photosynth. Res. 48*, 291−299.
38. Fernández-Velasco, J., and Crofts, A. R. (1991) *Biochem. Soc. Trans. 19*, 588−593.
39. Rott, M. A., Witthuhn, V. C., Schilke, B. A., Sorrano, M., Ali, A., and Donohue, T. J. (1993) *J. Bacteriol. 175*, 358−366.
40. Witthuhn, V. C., Gao, J., Hong, S., Halls, S., Rott, M. A., Wraight, C. A., Crofts, A. R., and Donohue, T. J. (1997) *Biochemistry 36*, 903−911.
41. Papiz, M. Z., Prince, S. M., HawthornthwaiteLawless, A. M., McDermott, G., Freer, A. A., Isaacs, N. W., and Cogdell, R. J. (1996) *Trends Plant Sci. 1*, 198−206.
42. Gray, K. A. M., and Daldal, F. (1995) in *Anoxygenic Photosynthetic Bacteria* (Blankenship, R. E., Madigan, M. T., and Bauer, C. E., Eds.) pp 747−774, Advances in Photosynthesis, Kluwer Academic Publishers, Dordrecht, The Netherlands.
43. Lilburn, T. G., Prince, R. C., and Beatty, J. T. (1995) *J. Bacteriol. 177*, 4593−4600.
44. Barz, W. P., Vermeglio, A., Francia, F., Venturoli, G., Melandri, B. A., and Oesterhelt, D. (1995) *Biochemistry 34*, 15248−15258.
45. McGlynn, P., Hunter, N., and Jones, M. R. (1994) *FEBS Lett. 349*, 349−353.
46. Yen, H. C., and Marrs, B. L. (1976) *J. Bacteriol. 126*, 619−629.
47. Davidson, E., Prince, R. C., Haith, C. E., and Daldal, F. (1989) *J. Bacteriol. 171*, 6059−6068.
48. Prince, R. C., and Daldal, F. (1987) *Biochim. Biophys. Acta 894*, 370−378.

BI973123D